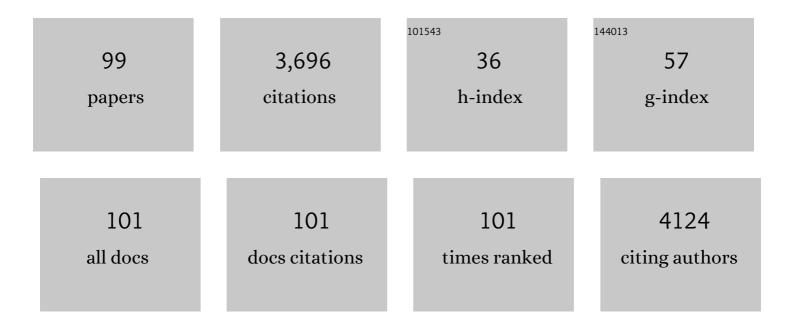
Yongchao Su

List of Publications by Year in descending order

Source: https://exaly.com/author-pdf/30333/publications.pdf Version: 2024-02-01



Υσνέςμλο Su

#	Article	IF	CITATIONS
1	Formulation and Processing Strategies which Underpin Susceptibility to Matrix Crystallization in Amorphous Solid Dispersions. Journal of Pharmaceutical Sciences, 2023, 112, 108-122.	3.3	11
2	Effect of Buffer Salts on Physical Stability of Lyophilized and Spray-Dried Protein Formulations Containing Bovine Serum Albumin and Trehalose. Pharmaceutical Research, 2023, 40, 1355-1371.	3.5	7
3	Investigating Crystalline Protein Suspension Formulations of Pembrolizumab from MAS NMR Spectroscopy. Molecular Pharmaceutics, 2022, 19, 936-952.	4.6	6
4	Optimization of Amorphization Kinetics during Hot Melt Extrusion by Particle Engineering: An Experimental and Computational Study. Crystal Growth and Design, 2022, 22, 821-841.	3.0	6
5	19F Solid-state NMR characterization of pharmaceutical solids. Solid State Nuclear Magnetic Resonance, 2022, 120, 101796.	2.3	10
6	Probing Molecular Packing of Drug Substances in Nanometer Domains in Pharmaceutical Formulations Using ¹⁹ F Magic Angle Spinning NMR. Journal of Physical Chemistry C, 2022, 126, 12025-12037.	3.1	4
7	Selective Nuclear Magnetic Resonance Method for Enhancing Long-Range Heteronuclear Correlations in Solids. Journal of Physical Chemistry Letters, 2022, 13, 6376-6382.	4.6	2
8	Design of Ternary Amorphous Solid Dispersions for Enhanced Dissolution of Drug Combinations. Molecular Pharmaceutics, 2022, 19, 2950-2961.	4.6	5
9	A novel amorphous solid dispersion based on drug–polymer complexation. Drug Delivery and Translational Research, 2021, 11, 2072-2084.	5.8	2
10	Antimicrobial Excipient-Induced Reversible Association of Therapeutic Peptides in Parenteral Formulations. Journal of Pharmaceutical Sciences, 2021, 110, 850-859.	3.3	3
11	Selective Laser Sintering 3-Dimensional Printing as a Single Step Process to Prepare Amorphous Solid Dispersion Dosage Forms for Improved Solubility and Dissolution Rate. Journal of Pharmaceutical Sciences, 2021, 110, 1432-1443.	3.3	44
12	Solid-state NMR spectroscopy in pharmaceutical sciences. TrAC - Trends in Analytical Chemistry, 2021, 135, 116152.	11.4	78
13	Probing Microenvironmental Acidity in Lyophilized Protein and Vaccine Formulations Using Solid-state NMR Spectroscopy. Journal of Pharmaceutical Sciences, 2021, 110, 1292-1301.	3.3	13
14	Understanding the Impact of Protein–Excipient Interactions on Physical Stability of Spray-Dried Protein Solids. Molecular Pharmaceutics, 2021, 18, 2657-2668.	4.6	24
15	Understanding molecular mechanisms of biologics drug delivery and stability from NMR spectroscopy. Advanced Drug Delivery Reviews, 2021, 174, 1-29.	13.7	40
16	Effect of Storage Humidity on Physical Stability of Spray-Dried Naproxen Amorphous Solid Dispersions with Polyvinylpyrrolidone: Two Fluid Nozzle vs. Three Fluid Nozzle. Pharmaceutics, 2021, 13, 1074.	4.5	5
17	Solubilizing temperature of crystalline drug in polymer carrier: A rheological investigation on a posaconazole-copovidone system with low drug load. European Journal of Pharmaceutics and Biopharmaceutics, 2021, 164, 28-35.	4.3	5
18	Solid-state NMR in the field of drug delivery: State of the art and new perspectives. Magnetic Resonance Letters, 2021, 1, 28-70.	1.3	9

#	Article	IF	CITATIONS
19	The effect of drug loading on the properties of abiraterone–hydroxypropyl beta cyclodextrin solid dispersions processed by solvent free KinetiSol® technology. European Journal of Pharmaceutics and Biopharmaceutics, 2021, 165, 52-65.	4.3	11
20	Formulating a heat- and shear-labile drug in an amorphous solid dispersion: Balancing drug deg degradation and crystallinity. International Journal of Pharmaceutics: X, 2021, 3, 100092.	1.6	6
21	Mechanistic Investigation of Drug Supersaturation in the Presence of Polysorbates as Solubilizing Additives by Solution Nuclear Magnetic Resonance Spectroscopy. Molecular Pharmaceutics, 2021, 18, 4310-4321.	4.6	4
22	Optimizing Solvent Selection and Processing Conditions to Generate High Bulk-Density, Co-Precipitated Amorphous Dispersions of Posaconazole. Pharmaceutics, 2021, 13, 2017.	4.5	16
23	In situ solidâ€ s tate NMR characterization of pharmaceutical materials: An example of drugâ€polymer thermal mixing. Magnetic Resonance in Chemistry, 2020, 58, 1049-1054.	1.9	6
24	Quantitative Analysis of Linker Composition and Spatial Arrangement of Multivariate Metal–Organic Framework UiO-66 through ¹ H Fast MAS NMR. Journal of Physical Chemistry C, 2020, 124, 17640-17647.	3.1	12
25	Quantifying Pharmaceutical Formulations from Proton Detected Solid-State NMR under Ultrafast Magic Angle Spinning. Journal of Pharmaceutical Sciences, 2020, 109, 3045-3053.	3.3	8
26	Selectively Enhanced ¹ H– ¹ H Correlations in Proton-Detected Solid-State NMR under Ultrafast MAS Conditions. Journal of Physical Chemistry Letters, 2020, 11, 8077-8083.	4.6	33
27	Quantifying Molecular Mixing and Heterogeneity in Pharmaceutical Dispersions at Sub-100 nm Resolution by Spin Diffusion NMR. Molecular Pharmaceutics, 2020, 17, 3567-3580.	4.6	26
28	Partial Dehydration of Levothyroxine Sodium Pentahydrate in a Drug Product Environment: Structural Insights into Stability. Molecular Pharmaceutics, 2020, 17, 3915-3929.	4.6	13
29	Toward Developing Discriminating Dissolution Methods for Formulations Containing Nanoparticulates in Solution: The Impact of Particle Drift and Drug Activity in Solution. Molecular Pharmaceutics, 2020, 17, 4125-4140.	4.6	12
30	Thermally Conductive Excipient Expands KinetiSol® Processing Capabilities. AAPS PharmSciTech, 2020, 21, 319.	3.3	14
31	Atomic-Level Drug Substance and Polymer Interaction in Posaconazole Amorphous Solid Dispersion from Solid-State NMR. Molecular Pharmaceutics, 2020, 17, 2585-2598.	4.6	28
32	Molecular Mechanism of Crystalline-to-Amorphous Conversion of Pharmaceutical Solids from ¹⁹ F Magic Angle Spinning NMR. Journal of Physical Chemistry B, 2020, 124, 5271-5283.	2.6	25
33	Molecular packing of pharmaceuticals analyzed with paramagnetic relaxation enhancement and ultrafast magic angle pinning NMR. Physical Chemistry Chemical Physics, 2020, 22, 13160-13170.	2.8	22
34	Understanding Molecular Interactions in Rafoxanide–Povidone Amorphous Solid Dispersions from Ultrafast Magic Angle Spinning NMR. Molecular Pharmaceutics, 2020, 17, 2196-2207.	4.6	29
35	Probing the Molecular-Level Interactions in an Active Pharmaceutical Ingredient (API) - Polymer Dispersion and the Resulting Impact on Drug Product Formulation. Pharmaceutical Research, 2020, 37, 94.	3.5	9
36	<i>In Vitro</i> and <i>In Vivo</i> Behaviors of KinetiSol and Spray-Dried Amorphous Solid Dispersions of a Weakly Basic Drug and Ionic Polymer. Molecular Pharmaceutics, 2020, 17, 2789-2808.	4.6	23

#	Article	IF	CITATIONS
37	Islatravir Case Study for Enhanced Screening of Thermodynamically Stable Crystalline Anhydrate Phases in Pharmaceutical Process Development by Hot Melt Extrusion. Molecular Pharmaceutics, 2020, 17, 2874-2881.	4.6	11
38	An Imaging Toolkit for Physical Characterization of Long-Acting Pharmaceutical Implants. Journal of Pharmaceutical Sciences, 2020, 109, 2798-2811.	3.3	8
39	Using thin film freezing to minimize excipients in inhalable tacrolimus dry powder formulations. International Journal of Pharmaceutics, 2020, 586, 119490.	5.2	39
40	Primary Adsorption Sites of Light Alkanes in Multivariate UiO-66 at Room Temperature as Revealed by Solid-State NMR. Journal of Physical Chemistry C, 2020, 124, 3738-3746.	3.1	12
41	Clay-Polymer Nanocomposites Prepared by Reactive Melt Extrusion for Sustained Drug Release. Pharmaceutics, 2020, 12, 51.	4.5	27
42	Advances of solidâ€state NMR spectroscopy in material sciences. Magnetic Resonance in Chemistry, 2020, 58, 987-987.	1.9	1
43	How broadly can poly(urethane)-based implants be applied to drugs of varied properties?. International Journal of Pharmaceutics, 2019, 568, 118550.	5.2	9
44	Can drug release rate from implants be tailored using poly(urethane) mixtures?. International Journal of Pharmaceutics, 2019, 557, 390-401.	5.2	12
45	Homogeneity of amorphous solid dispersions – an example with KinetiSol [®] . Drug Development and Industrial Pharmacy, 2019, 45, 724-735.	2.0	17
46	The peptide hormone glucagon forms amyloid fibrils with two coexisting β-strand conformations. Nature Structural and Molecular Biology, 2019, 26, 592-598.	8.2	58
47	Detecting and Quantifying Microscale Chemical Reactions in Pharmaceutical Tablets by Stimulated Raman Scattering Microscopy. Analytical Chemistry, 2019, 91, 6894-6901.	6.5	28
48	Three-Dimensional NMR Spectroscopy of Fluorinated Pharmaceutical Solids under Ultrafast Magic Angle Spinning. Analytical Chemistry, 2019, 91, 6217-6224.	6.5	38
49	Molecular Interactions in Posaconazole Amorphous Solid Dispersions from Two-Dimensional Solid-State NMR Spectroscopy. Molecular Pharmaceutics, 2019, 16, 2579-2589.	4.6	59
50	Influence of mechanical and thermal energy on nifedipine amorphous solid dispersions prepared by hot melt extrusion: Preparation and physical stability. International Journal of Pharmaceutics, 2019, 561, 324-334.	5.2	44
51	Enhanced Aerosolization of High Potency Nanoaggregates of Voriconazole by Dry Powder Inhalation. Molecular Pharmaceutics, 2019, 16, 1799-1812.	4.6	33
52	Understanding Compression-Induced Amorphization of Crystalline Posaconazole. Molecular Pharmaceutics, 2019, 16, 825-833.	4.6	28
53	Solid-state NMR analysis of crystalline and amorphous Indomethacin: An experimental protocol for full resonance assignments. Journal of Pharmaceutical and Biomedical Analysis, 2019, 165, 47-55.	2.8	29
54	A novel approach for measuring room temperature enthalpy of mixing and associated solubility estimation of a drug in a polymer matrix. Polymer, 2018, 135, 50-60.	3.8	9

Yongchao Su

#	Article	IF	CITATIONS
55	In Situ Stimulated Raman Scattering (SRS) Microscopy Study of the Dissolution of Sustained-Release Implant Formulation. Molecular Pharmaceutics, 2018, 15, 5793-5801.	4.6	30
56	The structure of a \hat{l}^22 -microglobulin fibril suggests a molecular basis for its amyloid polymorphism. Nature Communications, 2018, 9, 4517.	12.8	124
57	Quantifying Disproportionation in Pharmaceutical Formulations with ³⁵ Cl Solid-State NMR. Molecular Pharmaceutics, 2018, 15, 4038-4048.	4.6	28
58	Predicting physical stability of ternary amorphous solid dispersions using specific mechanical energy in a hot melt extrusion process. International Journal of Pharmaceutics, 2018, 548, 571-585.	5.2	47
59	Peptide and Protein Dynamics and Low-Temperature/DNP Magic Angle Spinning NMR. Journal of Physical Chemistry B, 2017, 121, 4997-5006.	2.6	60
60	Insights into Nano- and Micron-Scale Phase Separation in Amorphous Solid Dispersions Using Fluorescence-Based Techniques in Combination with Solid State Nuclear Magnetic Resonance Spectroscopy. Pharmaceutical Research, 2017, 34, 1364-1377.	3.5	49
61	Second harmonic generation microscopy as a tool for the early detection of crystallization in spray dried dispersions. Journal of Pharmaceutical and Biomedical Analysis, 2017, 146, 86-95.	2.8	22
62	Understanding the process-product-performance interplay of spray dried drug-polymer systems through complete structural and chemical characterization of single spray dried particles. Powder Technology, 2017, 320, 685-695.	4.2	35
63	In Situ Characterization of Pharmaceutical Formulations by Dynamic Nuclear Polarization Enhanced MAS NMR. Journal of Physical Chemistry B, 2017, 121, 8132-8141.	2.6	51
64	Rheology Guided Rational Selection of Processing Temperature To Prepare Copovidone–Nifedipine Amorphous Solid Dispersions via Hot Melt Extrusion (HME). Molecular Pharmaceutics, 2016, 13, 3494-3505.	4.6	52
65	Methanol carbonylation over copper-modified mordenite zeolite: A solid-state NMR study. Solid State Nuclear Magnetic Resonance, 2016, 80, 1-6.	2.3	26
66	Solid-State Spectroscopic Investigation of Molecular Interactions between Clofazimine and Hypromellose Phthalate in Amorphous Solid Dispersions. Molecular Pharmaceutics, 2016, 13, 3964-3975.	4.6	69
67	Rheological and solid-state NMR assessments of copovidone/clotrimazole model solid dispersions. International Journal of Pharmaceutics, 2016, 500, 20-31.	5.2	28
68	High Resolution Structural Characterization of Aβ ₄₂ Amyloid Fibrils by Magic Angle Spinning NMR. Journal of the American Chemical Society, 2015, 137, 7509-7518.	13.7	103
69	Lipid bilayer-bound conformation of an integral membrane beta barrel protein by multidimensional MAS NMR. Journal of Biomolecular NMR, 2015, 61, 299-310.	2.8	38
70	Paramagnetic relaxation enhancement solid-state NMR studies of heterogeneous catalytic reaction over HY zeolite using natural abundance reactant. Solid State Nuclear Magnetic Resonance, 2015, 66-67, 29-32.	2.3	8
71	Magic Angle Spinning Nuclear Magnetic Resonance Characterization of Voltage-Dependent Anion Channel Gating in Two-Dimensional Lipid Crystalline Bilayers. Biochemistry, 2015, 54, 994-1005.	2.5	34
72	Magic Angle Spinning NMR of Proteins: High-Frequency Dynamic Nuclear Polarization and ¹ H Detection. Annual Review of Biochemistry, 2015, 84, 465-497.	11.1	128

#	Article	IF	CITATIONS
73	Alteration of Interaction Between Astrocytes and Neurons in Different Stages of Diabetes: a Nuclear Magnetic Resonance Study Using [1-13C]Glucose and [2-13C]Acetate. Molecular Neurobiology, 2015, 51, 843-852.	4.0	18
74	Molecular Dynamics of Neutral Polymer Bonding Agent (NPBA) as Revealed by Solid-State NMR Spectroscopy. Molecules, 2014, 19, 1353-1366.	3.8	7
75	Secondary Structure in the Core of Amyloid Fibrils Formed from Human β ₂ m and its Truncated Variant ΔN6. Journal of the American Chemical Society, 2014, 136, 6313-6325.	13.7	40
76	Efficient, balanced, transmission line RF circuits by back propagation of common impedance nodes. Journal of Magnetic Resonance, 2013, 231, 32-38.	2.1	8
77	Cationic membrane peptides: atomic-level insight of structure–activity relationships from solid-state NMR. Amino Acids, 2013, 44, 821-833.	2.7	57
78	Interaction between Histidine and Zn(II) Metal Ions over a Wide pH as Revealed by Solid-State NMR Spectroscopy and DFT Calculations. Journal of Physical Chemistry B, 2013, 117, 8954-8965.	2.6	48
79	13C and 15N spectral editing inside histidine imidazole ring through solid-state NMR spectroscopy. Solid State Nuclear Magnetic Resonance, 2013, 54, 13-17.	2.3	11
80	Effect of input current modes on intermetallic layer and mechanical property of aluminum–steel lap joint obtained by gas metal arc welding. Materials Science & Engineering A: Structural Materials: Properties, Microstructure and Processing, 2013, 578, 340-345.	5.6	79
81	Expanding the Repertoire of Amyloid Polymorphs by Co-polymerization of Related Protein Precursors. Journal of Biological Chemistry, 2013, 288, 7327-7337.	3.4	36
82	Intramolecular 1H–13C distance measurement in uniformly 13C, 15N labeled peptides by solid-state NMR. Solid State Nuclear Magnetic Resonance, 2012, 45-46, 51-58.	2.3	4
83	Paramagnetic Cu(II) for Probing Membrane Protein Structure and Function: Inhibition Mechanism of the Influenza M2 Proton Channel. Journal of the American Chemical Society, 2012, 134, 8693-8702.	13.7	46
84	Conformational Disorder of Membrane Peptides Investigated from Solid-State NMR Line Widths and Line Shapes. Journal of Physical Chemistry B, 2011, 115, 10758-10767.	2.6	36
85	Structures of β-Hairpin Antimicrobial Protegrin Peptides in Lipopolysaccharide Membranes: Mechanism of Gram Selectivity Obtained from Solid-State Nuclear Magnetic Resonance. Biochemistry, 2011, 50, 2072-2083.	2.5	43
86	Structure and dynamics of cationic membrane peptides and proteins: Insights from solidâ€state NMR. Protein Science, 2011, 20, 641-655.	7.6	87
87	Orientation, Dynamics, and Lipid Interaction of an Antimicrobial Arylamide Investigated by ¹⁹ F and ³¹ P Solid-State NMR Spectroscopy. Journal of the American Chemical Society, 2010, 132, 9197-9205.	13.7	39
88	Membrane-Bound Dynamic Structure of an Arginine-Rich Cell-Penetrating Peptide, the Protein Transduction Domain of HIV TAT, from Solid-State NMR. Biochemistry, 2010, 49, 6009-6020.	2.5	92
89	Waterâ ^{~^} Protein Interactions of an Arginine-Rich Membrane Peptide in Lipid Bilayers Investigated by Solid-State Nuclear Magnetic Resonance Spectroscopy. Journal of Physical Chemistry B, 2010, 114, 4063-4069.	2.6	74
90	High-Resolution Orientation and Depth of Insertion of the Voltage-Sensing S4 Helix of a Potassium Channel in Lipid Bilayers. Journal of Molecular Biology, 2010, 401, 642-652.	4.2	34

#	Article	IF	CITATIONS
91	Extra-framework aluminium species in hydrated faujasite zeolite as investigated by two-dimensional solid-state NMR spectroscopy and theoretical calculations. Physical Chemistry Chemical Physics, 2010, 12, 3895.	2.8	92
92	Roles of Arginine and Lysine Residues in the Translocation of a Cell-Penetrating Peptide from ¹³ C, ³¹ P, and ¹⁹ F Solid-State NMR. Biochemistry, 2009, 48, 4587-4595.	2.5	131
93	Asymmetric Insertion of Membrane Proteins in Lipid Bilayers by Solid-State NMR Paramagnetic Relaxation Enhancement: A Cell-Penetrating Peptide Example. Journal of the American Chemical Society, 2008, 130, 8856-8864.	13.7	79
94	Reversible Sheet–Turn Conformational Change of a Cell-Penetrating Peptide in Lipid Bilayers Studied by Solid-State NMR. Journal of Molecular Biology, 2008, 381, 1133-1144.	4.2	41
95	BrÃ,nsted/Lewis Acid Synergy in Dealuminated HY Zeolite:  A Combined Solid-State NMR and Theoretical Calculation Study. Journal of the American Chemical Society, 2007, 129, 11161-11171.	13.7	349
96	Acidity of Mesoporous MoOx/ZrO2and WOx/ZrO2Materials:Â A Combined Solid-State NMR and Theoretical Calculation Study. Journal of Physical Chemistry B, 2006, 110, 10662-10671.	2.6	70
97	Acid sites and oxidation center in molybdena supported on tin oxide as studied by solid-state NMR spectroscopy and theoretical calculation. Physical Chemistry Chemical Physics, 2006, 8, 2378.	2.8	19
98	Acid sites in mesoporous Al-SBA-15 material as revealed by solid-state NMR spectroscopy. Microporous and Mesoporous Materials, 2006, 92, 22-30.	4.4	110
99	Combined DFT Theoretical Calculation and Solid-State NMR Studies of Al Substitution and Acid Sites in Zeolite MCM-22. Journal of Physical Chemistry B, 2005, 109, 24273-24279.	2.6	80